

Imaging of Ischemic but Viable Myocardium Using a New ^{18}F -Labeled 2-Nitroimidazole Analog, ^{18}F -FRP170

Tomohiro Kaneta, MD¹; Yoshihiro Takai, MD, PhD¹; Yutaka Kagaya, MD, PhD²; Yuriko Yamane, MD, PhD²; Hiroaki Wada, PhD³; Masahiro Yuki, PhD³; Ren Iwata, PhD³; Michihiko Tsujitani, PhD⁴; Shoki Takahashi, MD, PhD¹; and Shogo Yamada, MD, PhD¹

¹Department of Radiology, Tohoku University, Sendai, Japan; ²Department of Cardiovascular Medicine, Tohoku University, Sendai, Japan; ³Cyclotron and Radioisotope Center, Tohoku University, Sendai, Japan; and ⁴POLA Chemical Industries, Yokohama, Japan

RP170, 1-(2-hydroxy-1-[hydroxymethyl]ethoxy)methyl-2-nitroimidazole, is a new hypoxic radiosensitizer. We recently succeeded in labeling this compound with ^{18}F to make ^{18}F -FRP170, 1-(2-fluoro-1-[hydroxymethyl]ethoxy)methyl-2-nitroimidazole. In this study, we attempted to visualize the ischemic but viable myocardium of rats as hot-spot images using ^{18}F -FRP170. We also compared the distribution of ^{18}F -FRP170 with myocardial perfusion, fatty acid metabolism, and glucose metabolism.

Methods: In open-chest rats, the left coronary artery was ligated to make an ischemic myocardial model. We evaluated the myocardial accumulation of radiotracers by the double-tracer autoradiography technique. ^{14}C -Iodoantipyrine (IAP), ^{125}I -15-(*p*-iodophenyl)-3-(*R,S*)-methylpentadecanoic acid (BMIPP), and ^{14}C -deoxyglucose (DG) were used as markers of myocardial perfusion, fatty acid metabolism, and glucose metabolism, respectively. Approximately 80 small circular regions of interest were placed throughout the left ventricular wall of the midventricular level section. The uptake in each region of interest was expressed as the percentage uptake of the average count in the remote area. We then defined the ^{18}F -FRP170 high-uptake area (H-FRP) as that area where the percentage of FRP was $>120\%$ and the ^{18}F -FRP170 low-uptake area (L-FRP) as that area where the percentage of FRP was $<80\%$. **Results:** On the ^{18}F -FRP170 image of the ischemic myocardium, there was a low-uptake area in the center, which was bounded by a high-uptake area. The percentages of IAP in the H-FRP and the L-FRP were $48.5\% \pm 5.8\%$ and $2.2\% \pm 0.2\%$, respectively; the percentages of BMIPP in the H-FRP and the L-FRP were $46.8\% \pm 3.1\%$ and $4.3\% \pm 0.4\%$, respectively; and the percentages of DG in the H-FRP and the L-FRP were $107.0\% \pm 6.8\%$ and $4.3\% \pm 0.4\%$, respectively. In diabetic rats, the percentages of DG in the H-FRP and the L-FRP were $407.7\% \pm 14.9\%$ and $72.5\% \pm 5.0\%$, respectively, but the remote area on the DG image was insufficiently visualized. Histologic data using 2,3,5-triphenyltetrazolium chloride staining suggest that the high-uptake areas on ^{18}F -FRP170 images reflect ischemic but viable myocardium. **Conclusion:** We succeeded in visualizing the ischemic but viable myocardium as a hot spot on the ^{18}F -

FRP170 image. ^{18}F -FRP170 can be expected to provide important information for determining the necessity of coronary intervention in ischemic heart disease patients, including diabetic patients.

Key Words: 2-nitroimidazole; RP170; ischemia; myocardium; autoradiography

J Nucl Med 2002; 43:109–116

The 2-nitroimidazoles were developed as selective radiosensitizers of hypoxic cells and are used as adjuvants to radiotherapy in the treatment of malignant tumors (1). They have an interesting property—namely, they accumulate selectively in hypoxic cells. The mechanism for the intracellular retention in hypoxic cells is not fully understood. It is believed that 2-nitroimidazoles undergo nitro-reduction with the formation of products that bind to intracellular elements and remain trapped in hypoxic tissues. The enzymatic nitro-reduction required for trapping does not occur unless the cell is viable (2). Therefore, nitroimidazoles increasingly accumulate in the viable area, but not in the necrotic area, of the ischemic myocardium.

In 1981, it was suggested that radiolabeled 2-nitroimidazoles could be used for the direct visualization of tissue hypoxia in tumors (3). ^{18}F -Fluoromisonidazole was the first such radiopharmaceutical developed (4,5), and then many types of radiolabeled 2-nitroimidazoles were synthesized subsequently (6–8). These compounds have been applied to myocardial imaging. Compounds characterized by high lipophilicity were thought to be better for imaging hypoxia because increased lipophilicity results in increased uptake into the myocytes (9). However, the hepatocellular uptake and retention also increases. Moreover, the blood clearance becomes slow and the contrast between the blood pool and the organs of interest decreases (10). These factors complicate *in vivo* imaging of myocardial hypoxia or ischemia. Recently, efforts have been directed toward reducing li-

Received Mar. 27, 2001; revision accepted Sep. 25, 2001.
For correspondence or reprints contact: Shogo Yamada, MD, PhD, Department of Radiology, Tohoku University School of Medicine, 1-1 Seiryomachi, Aoba-ku, Sendai 980-8574, Japan.
E-mail: shogo-y@rad.med.tohoku.ac.jp

pophilicity (11–15). RP170 (16), 1-(2-hydroxy-1-[hydroxymethyl]ethoxy)methyl-2-nitroimidazole, is a compound that reduces lipophilicity. It was developed and kindly provided by POLA Chemical Industries (Yokohama, Japan). Its octanol–water partition coefficient is 0.094 versus 0.35 for misonidazole and ~40 for BMS181321 (15,16).

We recently succeeded in labeling RP170 with ^{18}F to make ^{18}F -FRP170, 1-(2-fluoro-1-[hydroxymethyl]ethoxy)methyl-2-nitroimidazole (17). The change in lipophilicity induced by fluorinating is undetermined, but ^{18}F -FRP170 is expected to have low lipophilicity and to show higher-contrast images with a low background level.

In this study, we attempted to determine whether ^{18}F -FRP170 could be used to visualize the ischemic but viable myocardium as a hot-spot image using the double-tracer autoradiographic technique with a perfusion marker. Moreover, we compared the distribution of ^{18}F -FRP170 with those of ^{125}I -15-(*p*-iodophenyl)-3-(*R,S*)-methylpentadecanoic acid (BMIPP) and ^{14}C -deoxyglucose (DG). BMIPP is a marker of fatty acid metabolism and is believed to be a more direct index of regional ischemia than the perfusion markers ^{201}Tl and $^{99\text{m}}\text{Tc}$ -sestamibi. DG is considered to be the gold standard for detecting the ischemic viable myocardium. Finally, we compared the usefulness of this new agent with that of DG under the conditions of diabetes mellitus.

MATERIALS AND METHODS

This study was performed in conformance with the guidelines of the National Institutes of Health for Care and Use of Laboratory Animals and with the approval of the Committee of Animal Experiments at the Cyclotron and Radioisotope Center of Tohoku

University. Male Wistar rats (Funabashi Farms, Shizuoka, Japan; body weight, 180–200 g) were used in these studies. They were fed normal rat chow and had tap water ad libitum until they were subjected to the surgical procedure. As an exception, rats in groups 3 and 4 (comparison with glucose metabolism) were subjected to fasting at 12 PM on the day of surgery. We started the surgical procedure at approximately 6 PM. Rats were anesthetized with an intraperitoneal injection of sodium pentobarbital (40 mg/kg) and mechanically ventilated after endotracheal intubation. The right jugular vein was cannulated with a PE-50 polyethylene tube for the injection of radiopharmaceuticals. A left-sided thoracotomy was performed through the fifth intercostal space. A ligature was placed around the left coronary artery (LCA) near its origin using a 6-0 silk suture. To prevent ventricular arrhythmias, 1 mg/kg lidocaine was injected before the LCA was ligated. In this ischemic model, the septum is not subjected to ischemia (18–21). Therefore, we defined the remote area as the nonischemic area in the septum. Three types of double-tracer autoradiography using ^{18}F -FRP170 and other radiotracers were performed as detailed below. Each experimental protocol (protocols 1–4) is summarized in Figure 1.

In group 1 ($n = 3$), a comparison with a myocardial perfusion marker was performed using protocol 1. ^{18}F -FRP170 (55.5 MBq), with a specific activity of >26 GBq/ μmol , was injected intravenously 30 min after the LCA ligation. Fifteen minutes after the injection of ^{18}F -FRP170, 4-*N*-methyl- ^{14}C -iodoantipyrine ([IAP] 0.185 MBq), with a specific activity of 188 GBq/nmol, dissolved in 1.6 mL 0.9% NaCl, was injected intravenously for 30 s at a constant rate with an infusion pump. Immediately after the end of ^{14}C -IAP infusion, the rats were killed by severing the ascending aorta and the pulmonary trunk. The hearts were excised rapidly and frozen in dry ice.

In group 2 ($n = 5$), a comparison with aerobic fatty acid metabolism was performed using protocol 2. ^{125}I -BMIPP was obtained from Nihon Medi-Physics Co., Ltd. (Nishinomiya, Ja-

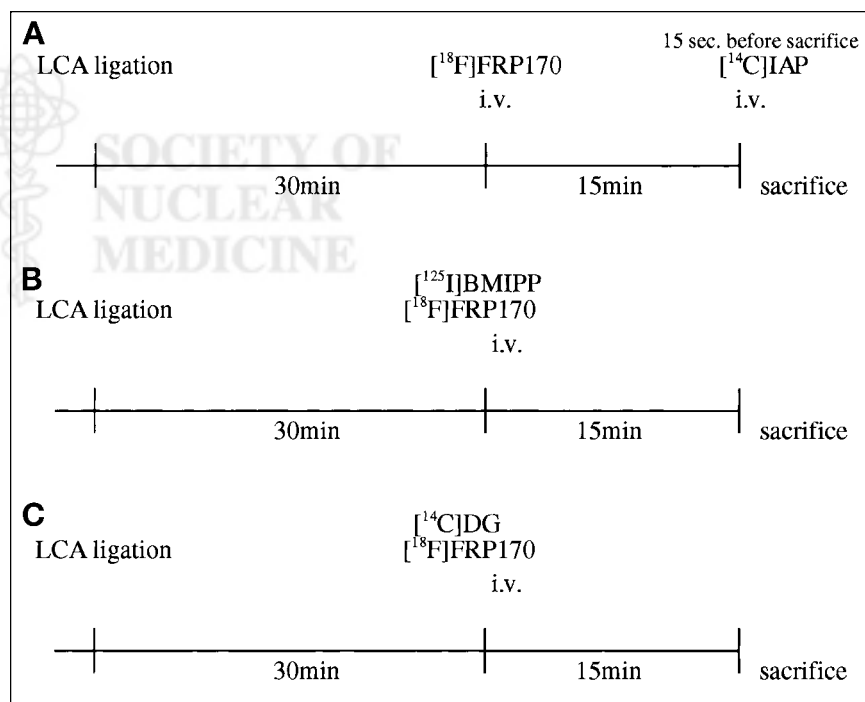


FIGURE 1. Experimental protocols. (A) Protocol 1: ^{18}F -FRP170 and ^{14}C -IAP. (B) Protocol 2: ^{18}F -FRP170 and ^{125}I -BMIPP. (C) Protocol 3: ^{18}F -FRP170 and ^{14}C -DG. i.v. = intravenous injection.

pan). Thirty minutes after the LCA ligation, 55.5 MBq ^{18}F -FRP170 and 185 kBq ^{125}I -BMIPP with a specific activity of 710 MBq/mol were injected intravenously. Fifteen minutes after the injection, the rats were killed and the hearts were excised rapidly and frozen in dry ice.

In group 3 ($n = 5$), a comparison with anaerobic glucose metabolism was performed using protocol 3. ^{14}C -DG was obtained from Amersham International PLC. (Buckinghamshire, U.K.). Thirty minutes after the LCA ligation, 55.5 MBq ^{18}F -FRP170 and 185 kBq ^{14}C -DG with a specific activity of 2.11 GBq/mol were injected intravenously. Fifteen minutes after the injection, the rats were killed and the hearts were excised rapidly and frozen in dry ice.

In group 4 ($n = 5$), the same protocol as that used for group 3 was performed on streptozotocin-induced diabetic rats. The rats were administered streptozotocin (45 mg/kg of body weight) intravenously 5 d before the surgical procedure. The plasma glucose level was measured by using a Precision QID monitor (MediSense, Bedford, MA), and the plasma insulin level was measured by a rat insulin ^{125}I assay system (Amersham Pharmacia Biotech, Buckinghamshire, U.K.).

Double-Tracer Autoradiography

Approximately 30 frozen heart sections (20 μm thick), taken perpendicular to the long axis of the left ventricle, were prepared. The sections were placed in contact with general-use imaging plates (SR2025; Fuji Photo Film Co., Ltd., Kanazawa, Japan). The first autoradiographic exposure for 1 h detected the distribution of ^{18}F -FRP170. The ^{18}F was allowed to decay for 20 h, and then ^{14}C and ^{125}I images were obtained by a second exposure for 1 and 3 wk, respectively. By single-tracer autoradiography using ^{14}C -IAP, ^{125}I -BMIPP, and ^{14}C -DG, we initially confirmed that these agents were not visualized under conditions applicable for ^{18}F -FRP170 imaging.

One representative autoradiogram per animal with the largest cross-sectional area of the left ventricle was analyzed by a computerized imaging analysis system (Bio-Imaging Analyzer BAS5000; Fuji Photo Film Co.). The image data were recorded as the digitized values (photostimulated luminescence [PSL]) of each pixel (50 \times 50 μm) in the analyzing unit of this system (18). Approximately 80 circular regions of interest (ROIs) (the area of each ROI was approximately 0.1 mm^2) were placed on the ^{18}F -FRP170 image throughout the left ventricular wall of the midventricular level section. We put the ROIs on the other image at the same sites as the ^{18}F -FRP170 images using the traced film. The uptake values in each ROI were expressed as the autoradiographic intensities ($[\text{PS} - \text{BG}]/\text{A}$), where $\text{BG} = \text{PSL}$ of the background and $\text{A} = \text{area}$ (mm^2). We determined the percentage uptake values in each tracer's image with the average ($[\text{PSL} - \text{BG}]/\text{A}$) of the remote area assumed to be 100. The percentage of FRP was determined from the ^{18}F -FRP170 image, percentage of IAP from the ^{14}C -IAP image, percentage of BMIPP from the ^{125}I -BMIPP image, and percentage of DG from the ^{14}C -DG image. The mean SD of the percentage of FRP in the remote area of group 1 ($n = 3$) was 10.19%. Because the value of 2 SD was approximately 20%, we defined the ^{18}F -FRP170 high-uptake area (H-FRP) as that area where the percentage of FRP was $>120\%$ and the ^{18}F -FRP170 low-uptake area (L-FRP) as that area where the percentage of FRP was $<80\%$.

Histologic Examination

To confirm that the ischemic but viable myocardium identified by ^{18}F -FRP170 and ^{14}C -DG images is consistent with that determined by a widely accepted histologic method, 2,3,5-triphenyltetrazolium chloride (TTC) (Sigma Chemical Co., St. Louis, MO) staining, we performed an additional experiment using 3 rats. In this protocol, the suture for the LCA ligation was released 30 min after the onset of ischemia. The chest was closed, and rats were allowed to recover for 24 h. We reperfused those hearts because TTC staining requires >2 h after the onset of ischemia to identify precisely necrotic tissue and viable myocardium (22). Those rats were anesthetized again and intubated for artificial ventilation, and the LCA was ligated at the same position as the first ligation. To delineate the risk area, we injected 5 mL 1.0% Evans blue (Sigma Chemical) from the apex of each left ventricle. The hearts were then isolated, washed with saline, and cut into 5 transverse slices. The slices were incubated with 1.5% TTC solution for 15 min at 36°C and then photographed.

Statistical Analysis

Data are presented as mean \pm SE. Comparison between the regions was done using ANOVA with a multiple comparison test. $P < 0.05$ was considered significant.

RESULTS

Figure 2 shows representative autoradiograms of the midventricular heart sections obtained in all protocols. Circumferential profile curves of every 2 radiotracers used in protocols 1, 2, and 3 are shown in Figure 3. Figures 3A, 3B, and 3C correspond to Figures 2A, 2B, and 2C, respectively. Table 1 summarizes the percentages of IAP, BMIPP, and DG in the H-FRP and the L-FRP.

Comparison with Myocardial Perfusion

Figure 2A shows that the distribution of ^{18}F -FRP170 and ^{14}C -IAP in the remote area is homogeneous. On the other hand, the distribution of ^{18}F -FRP170 is increased at the edge of the ischemic area, although the distribution of ^{14}C -IAP is decreased in almost the whole area of the free wall. Representative circumferential profile curves of the percentages of FRP and IAP are shown in Figure 3A. In the path from the septum to the center of the free wall, the increase in ^{18}F -FRP170 uptake starts almost at the same position as where ^{14}C -IAP uptake decreases. The ^{18}F -FRP170 uptake decreases in the center of the free wall below the uptake in the remote area. Table 1 shows that ^{14}C -IAP distribution was significantly lower in the H-FRP and the L-FRP than in the remote area. The percentages of IAP in the H-FRP and the L-FRP were $48.5\% \pm 5.8\%$ and $2.2\% \pm 0.2\%$, respectively (Table 1).

Comparison with Fatty Acid Metabolism

Figure 2B shows that the uptake of ^{125}I -BMIPP decreased in the free wall, especially in the center. According to the representative circumferential profile curves in Figure 3B, the increase in ^{18}F -FRP170 uptake started at almost the same position as where ^{125}I -BMIPP uptake decreased. The ^{18}F -FRP170 uptake decreased in the center of the free wall

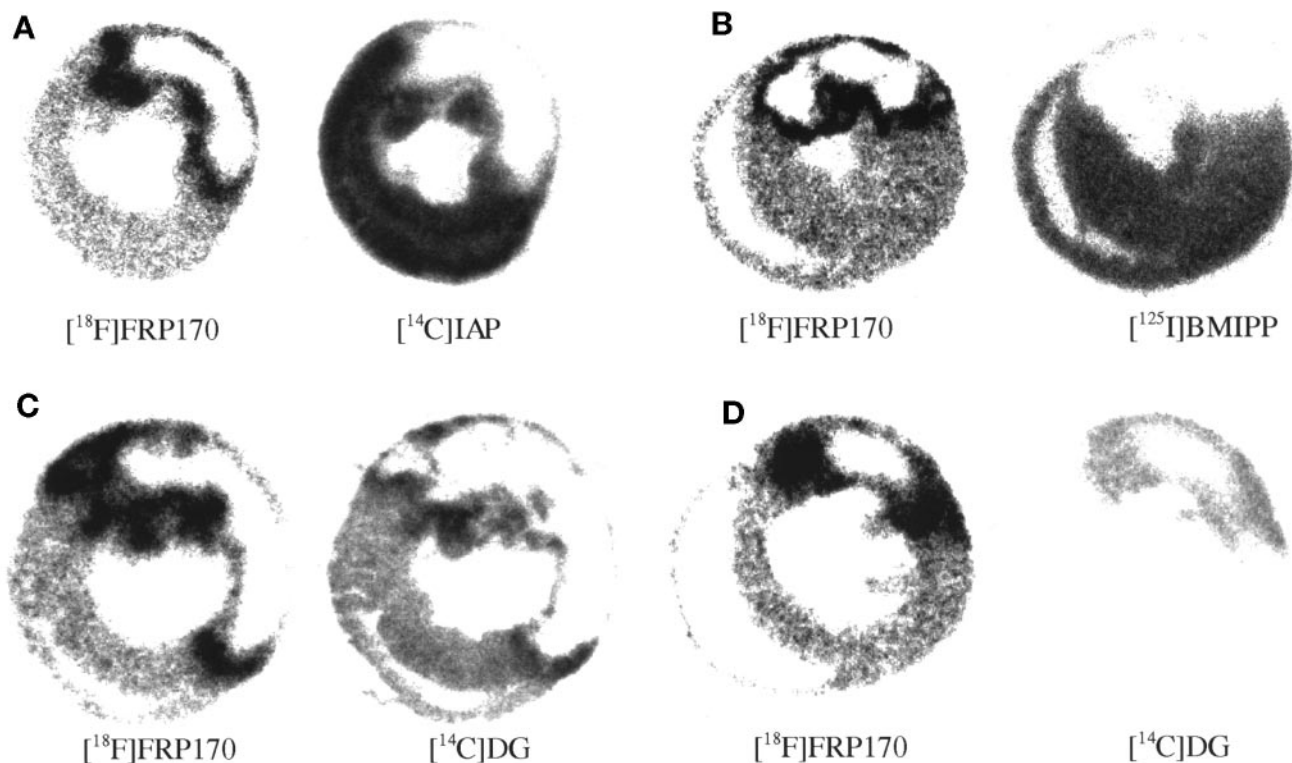


FIGURE 2. Representative double-tracer autoradiograms obtained from each protocol. All coupled autoradiograms were obtained from same slice. In each group, autoradiograms on left show ^{18}F -FRP170 image. Autoradiograms on right show image with ^{14}C -IAP as marker of myocardial perfusion (A), ^{125}I -BMIPP as marker of myocardial fatty acid metabolism (B), and ^{14}C -DG as marker of myocardial glucose metabolism in slice obtained from heart of nondiabetic rat (C) and slice obtained from heart of diabetic rat (D). Autoradiograms on right were expressed at same window level and width.

below the uptake in the remote area. Table 1 shows that ^{125}I -BMIPP has a significantly lower distribution in the H-FRP and the L-FRP than in the remote area. The percentages of BMIPP in the H-FRP and the L-FRP were $46.8\% \pm 3.1\%$ and $4.3\% \pm 0.4\%$, respectively (Table 1).

Comparison with Glucose Metabolism

We did not measure the glucose and insulin levels of rats subjected to autoradiographic study in group 3 because blood sampling may elicit hemodynamic deterioration. However, in our preliminary experiment, we determined those levels in open-chest and artificially ventilated rats ($n = 30$) in the same feeding state. The concentrations of glucose and insulin were 218 ± 8 mg/mL and 8.29 ± 0.81 ng/mL, respectively.

Figure 2C shows autoradiograms of ^{18}F -FRP170 and ^{14}C -DG. In the left ventricular free wall, there is a low-uptake area that is bounded by the high-uptake area on both autoradiograms. However, the area of increased ^{18}F -FRP170 uptake is slightly broader than that of ^{14}C -DG. According to the representative circumferential profile curves in Figure 3C, the increase in ^{18}F -FRP170 uptake started at almost the same position as where ^{14}C -DG uptake increased. But the decrease in ^{14}C -DG uptake started closer to the remote area

than the point where ^{18}F -FRP170 uptake started decreasing. The percentages of DG in the H-FRP and the L-FRP were $107.0\% \pm 6.8\%$ and $4.3\% \pm 0.4\%$, respectively (Table 1)—namely, the percentage of DG in the H-FRP exceeded 100% but did not reach 120%. On all autoradiograms in this protocol, the maximum percentages of FRPs were higher than the maximum percentages of DGs ($257.6\% \pm 16.7\%$ vs. $187.2\% \pm 22.1\%$; $n = 5$, $P < 0.01$).

Comparison with Glucose Metabolism in Diabetic Rats

The plasma glucose level of the diabetic rats was 368 ± 11 mg/dL and the plasma insulin level was 0.275 ± 0.041 ng/mL. Figure 2D shows the ^{14}C -DG image of diabetic rats, with the autoradiogram expressed at the same window level and width as the ^{14}C -DG image in Figure 2C. The ^{14}C -DG uptake in Figure 2D is very low, especially in the remote area. The distribution of ^{18}F -FRP170 was similar in nondiabetic and diabetic rats. The percentages of DG in the H-FRP and the L-FRP in diabetic rats were $407.7\% \pm 14.9\%$ and $72.5\% \pm 5.0\%$, respectively (Table 1). These values were extremely high compared with any values for nondiabetic rats. The maximum percentage of DG in diabetic rats was higher than the maximum percentage of FRP attributed to the extremely low DG uptake in the remote

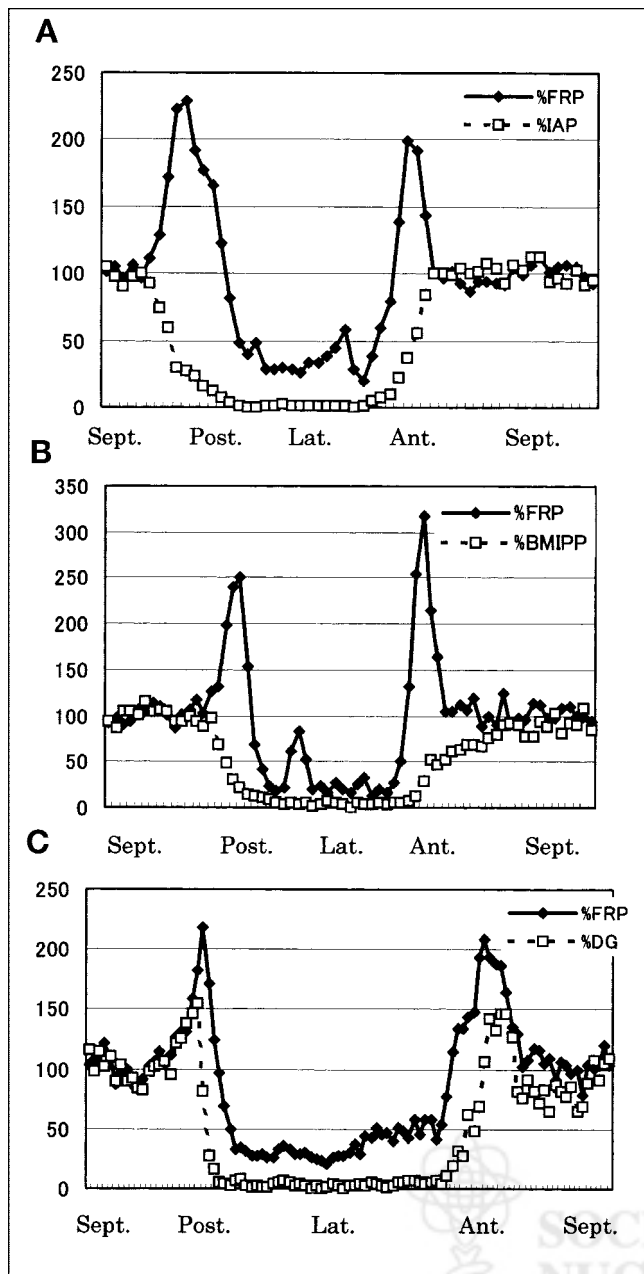


FIGURE 3. Circumferential profile curves of 2 radiotracers used in protocols 1, 2, and 3. (A) ^{18}F -FRP170 and ^{14}C -IAP. (B) ^{18}F -FRP170 and ^{125}I -BMIPP. (C) ^{18}F -FRP170 and ^{14}C -DG. ROIs were placed in serial order in midmyocardial layer of left ventricular wall. Sept. = septum; Post. = posterior; Lat. = lateral; Ant. = anterior.

area because the percentage of DG in the diabetic rats was only a few times as high as the background level. Table 2 shows the autoradiographic intensities expressed by $(\text{PSL} - \text{BG})/\text{A}$ in all regions of the ischemic hearts of normal and diabetic rats. The ^{14}C -DG uptake values of the ischemic hearts of diabetic rats were extremely low compared with those of nondiabetic rats. However, the ^{18}F -

TABLE 1
Regional Percentage Uptake Values Compared with Remote Area

Area	Group 1 (% ^{14}C -IAP)	Group 2 (% ^{125}I -BMIPP)	Group 3 (% ^{14}C -DG)	Group 4* (% ^{14}C -DG)
H-FRP	48.5 ± 5.8	46.8 ± 3.1	107.0 ± 6.8	407.7 ± 14.9
L-FRP	2.2 ± 0.2	4.3 ± 0.4	4.3 ± 0.4	72.5 ± 5.0

*Diabetic rats.

Average percentage uptake values (^{18}F -FRP, ^{125}I -BMIPP, and ^{14}C -DG) were calculated with average uptake of remote area assumed to be 100. There were significant differences between 2 areas in every group ($P < 0.0001$, Scheffé test). Values are mean ± SE.

FRP170 uptake values did not show such a remarkable difference between rats with and without diabetes mellitus.

Histologic Correlations

Figure 4 shows a representative TTC-stained section of a heart subjected to 30 min of LCA ligation followed by 24 h of reperfusion. Viable myocardium (stained red) is located at the periphery of the risk area, and necrotic myocardium (pale) is at the center. The distribution of viable myocardium identified by TTC staining is similar to that determined by ^{18}F -FRP170 and ^{14}C -DG images.

DISCUSSION

We successfully visualized ischemic but viable myocardium using ^{18}F -FRP170 in rats. It was possible to compare ^{18}F -FRP170 images with the images obtained by the double-tracer autoradiography technique using ^{14}C -IAP, ^{125}I -BMIPP, or ^{14}C -DG. In recent studies of hypoxic markers for ischemic myocardium using the coronary artery occlusion/reperfusion heart model, the timing of the injection of radiotracers was often discussed. Fukuchi et al. (19) reported that the uptake of BMS181321 in the area at risk was increased significantly only when BMS181321 was injected before ischemia. Johnson et al. (23) reported that focal

TABLE 2
Comparison of Autoradiographic Intensities Between Nondiabetic and Diabetic Rats

Area	^{18}F -FRP170		^{14}C -DG	
	Nondiabetic	Diabetic	Nondiabetic	Diabetic
Remote	395.0 ± 18.3	373.7 ± 9.9	459.2 ± 28.3	53.2 ± 4.3
H-FRP	755.5 ± 60.6	781.0 ± 38.6	564.6 ± 35.6	224.6 ± 12.9
L-FRP	143.5 ± 20.4	145.7 ± 9.5	17.1 ± 2.0	34.0 ± 2.4

Autoradiographic intensities are expressed by $(\text{PSL} - \text{BG})/\text{A}$. ^{14}C -DG uptake values in ischemic hearts of diabetic rats were extremely low compared with those of nondiabetic rats; ^{18}F -FRP170 uptake values showed much less variance. Values are mean ± SE.



FIGURE 4. Representative TTC-stained section of heart subjected to 30 min of LCA ligation followed by 24 h of reperfusion. Dark area represents nonischemic area stained with Evans blue. Viable myocardium in risk area (red) is located at periphery and necrotic myocardium (pale) is at center of risk area.

increased uptake of ^{99m}Tc -nitroheterocycle was seen in the risk region in animals injected 5 and 2.2 min before occlusion but not in animals injected 15 min before occlusion and 15 min after reperfusion. On the basis of the known kinetics of delivery and nitroimidazole reduction, these agents have not been considered to be useful for the detection of transient ischemia (2). Therefore, because we used only an acute ischemic heart model without reperfusion, our new hypoxic marker was injected after occlusion. On ^{18}F -FRP170 images of the free wall of the left ventricle, there was an area with higher uptake than that of the remote area and an area with lower uptake than that of the remote area. A comparison of ^{18}F -FRP170 images with ^{14}C -IAP images showed that the ^{18}F -FRP170 H-FRP and L-FRP were located in the low-perfusion area. When cells have an increased accumulation of ^{18}F -FRP170, it means that they are hypoxic but viable, which was confirmed by the TTC staining in this study. Therefore, the H-FRP on ^{18}F -FRP170 images reflects the ischemic viable myocardium. To be exact, we succeeded in visualizing the ischemic but viable myocardium as a hot spot on the ^{18}F -FRP170 image. These areas were located in a relatively mild ischemic area, but the region of the ischemic viable myocardium could not be detected by perfusion images alone.

^{125}I -BMIPP images showed a tendency that was similar to that of previous perfusion images. High- and low-uptake

areas on the ^{18}F -FRP170 images were located in the decreased-uptake area on the ^{125}I -BMIPP images. BMIPP is a radioiodinated methyl-branched fatty acid. Under aerobic conditions, the oxidation of fatty acids is the most important source of energy in the form of adenosine triphosphate (24). On the other hand, under ischemic hypoxic conditions, the oxidation of long-chain fatty acids is suppressed, with augmentation of glucose utilization (25–27). Lack of oxygen rapidly depresses β -oxidation, and activated fatty acids are shunted into storage pools as triglycerides and phospholipids (28). In addition, backdiffusion of unmetabolized fatty acids increases significantly because the ischemic tissue is no longer able to activate and trap them. Therefore, the autoradiographic findings of a moderate decrease in ^{125}I -BMIPP uptake in the ^{18}F -FRP170 H-FRP and a severe decrease in the uptake in the ^{18}F -FRP170 L-FRP correspond to cardiac fatty acid metabolism depending on the intracellular partial pressure of oxygen. To our knowledge, no previous study has reported a correlation between the markers of hypoxia and fatty acid metabolism in the ischemic myocardium.

We also studied the correlation between ^{18}F -FRP170 and ^{14}C -DG in the ischemic myocardium using nondiabetic and diabetic rats. In nondiabetic rats, the area with increased ^{18}F -FRP170 uptake was broader and more prominent than the area with increased uptake of ^{14}C -DG. These results suggest that ^{18}F -FRP170 is as useful as DG in detecting ischemic viable myocardium and that the broader hot spots and higher maximum percentage of uptake on ^{18}F -FRP170 images than on ^{14}C -DG images may lead to easier detection of them, especially in the clinical setting using PET.

Much of the increase in glucose metabolism of acute ischemic myocardial cells is caused by the translocation of GLUT4 molecules known as insulin-responsive glucose transporters (29). The conditions or stimuli that are now known to induce glucose transporters in the heart include insulin (30–33), catecholamines (34), increased workload (35), hypoxia (30), and ischemia. Therefore, in this study, the increased uptake of DG in the myocardium is also believed to be caused by the translocation of glucose transporters induced by ischemia or hypoxia (or both). Decreases in the GLUT4 content in the heart have been reported in diabetic rats (36). The glucose transport in response to physiologic stimuli has also been reported to be impaired in diabetic rats (37). In our study, the percentages of DG in the H-FRP and L-FRP were found to be much higher than those in other studies. This finding must be attributed to the remarkably decreased ^{14}C -DG uptake in the remote area. One of the mechanisms for the low DG uptake in the diabetic hearts, especially in the remote area, is thought to be the low level of serum insulin. The uptake of ^{14}C -DG in the remote area of diabetic rats is only several times as high as the background level, which may make it difficult to recognize the anatomic structure of the heart and to deter-

mine where the lesion is. On the other hand, the pattern of ^{18}F -FRP170 uptake in the ischemic heart of diabetic rats was the same as that of nondiabetic rats. The ^{18}F -FRP170 images do not seem to be influenced by the presence of diabetes mellitus.

In this study, we showed that direct hot-spot imaging of ischemic but viable myocardium was possible using a newly developed 2-nitroimidazole analog (i.e., ^{18}F -FRP170). This direct hot-spot imaging is potentially of great clinical importance. If the ischemic but viable myocardium can be detected, we could select appropriate candidates for percutaneous interventional treatment or coronary artery bypass grafting. ^{18}F -FDG PET is currently considered to be the gold standard for the assessment of myocardial viability. However, our results suggest that ^{18}F -FRP170 is as useful as ^{18}F -FDG for detecting the ischemic viable myocardium. Furthermore, in this study, the ^{18}F -FRP170 uptake in the ischemic viable myocardium was broader and higher than that of DG. This might enable an easier detection of ischemic viable myocardium than that by FDG in the clinical setting using PET. Finally, ^{18}F -FRP170 may be more useful in diabetic patients than ^{18}F -FDG because the images seem to be independent of the existence of diabetes mellitus. An advantage of this new agent might be that there is no requirement for glucose loading or consideration of the meal plan even in nondiabetic patients. FDG imaging after overnight fasting may possibly show ischemic myocardium as a hot spot. However, we showed previously that stimulated DG uptake in the ischemic border zone still depends on the DG uptake in the nonischemic remote area (21). The FDG uptake in the ischemic myocardium after overnight fasting might be only a relative hot spot but not a prominent hot spot.

This study has some limitations. First, our results showed that the area with increased uptake of ^{18}F -FRP170 was broader (reached to the central ischemic area) and more prominent than the area with increased uptake of ^{14}C -DG. However, we do not know whether this observation indicates that ^{18}F -FRP170 is more sensitive than DG in detecting ischemic viable myocardium or that this new agent overestimates it. We could not perform TTC staining using the same slices of hearts as those used for ^{18}F -FRP170 or ^{14}C -DG imaging because, in this study, reperfusion was mandatory for TTC staining to avoid overestimation of viable myocardium. Further investigation is necessary to address this question, although the difference in the size of ischemic viable areas determined by ^{18}F -FRP170 and ^{14}C -DG was not large. Second, in this study, we used ^{18}F -FRP170 to successfully visualize ischemic but viable myocardium only ex vivo. When we consider the application of ^{18}F -FRP170 to the clinical setting using PET, we have to consider the feasibility of myocardial imaging with ^{18}F -FRP170 in vivo. In this regard, we need to know the ratio of the myocardial count to the blood count, which was not available in this study.

CONCLUSION

In this study, we succeeded in synthesizing a new positron-labeled 2-nitroimidazole analog, ^{18}F -FRP170. This radiopharmaceutical appears to be useful in the same way as DG for detecting ischemic viable myocardium. ^{18}F -FRP170 PET images may be suitable for quantitative evaluation of ischemic viable myocardium and for accurate diagnosis of acute myocardial infarction. However, because experimental studies are not an adequate basis on which to make general conclusions concerning the possible clinical application, further investigations are warranted.

ACKNOWLEDGMENTS

The authors thank Drs. Tatsuo Ido, Hiroshi Fukuda, and Kazuo Kubota for their thoughtful suggestions. This work was supported by a grant from the Association for Nuclear Technology in Medicine (Tokyo, Japan).

REFERENCES

1. Franko A. Misonidazole and other hypoxia markers: metabolism and applications. *Int J Radiat Oncol Biol Phys.* 1986;12:1195-1202.
2. Nunn A, Linder K, Strauss HW. Nitroimidazole and imaging hypoxia. *Eur J Nucl Med.* 1995;22:265-280.
3. Chapman J, Franko A, Sharplin J. A marker of hypoxic cells in tumors with potential clinical applicability. *Br J Cancer.* 1981;43:546-550.
4. Jerabeck PA, Patrick TB, Kilbourn MR, et al. Synthesis and biodistribution of ^{18}F -labeled fluoronitroimidazoles: potential in vivo markers of hypoxic tissue. *Int J Radiat Appl Instrum [A].* 1986;37:599-605.
5. Martin GV, Caldwell JH, Graham MM, et al. Non-invasive detection of hypoxic myocardium using fluorine-18-fluoromisonidazole and positron emission tomography. *J Nucl Med.* 1992;33:2202-2208.
6. Biskupiak JE, Grierson JR, Rasey JS, Martin GV, Krohn KA. Synthesis of an (iodovinyl)misonidazole derivative for hypoxia imaging. *J Med Chem.* 1991;34:2165-2168.
7. Mannan RH, Somayaji VV, Lee J, Mercer JR, Chapman JD, Wiebe LI. Radioiodinated 1-(5-iodo-5'-deoxy-D-arabinofuranosyl)-2-nitroimidazole (iodoazomycin arabinoside: IAZA): a novel marker of tissue hypoxia. *J Nucl Med.* 1991;32:1764-1770.
8. Linder KE, Chan Y-W, Cyr JE, Malley MF, Nowotnik DP, Nunn AD. TcO-(PnA.O-1-(2-nitroimidazole)) [BMS181321], a new technetium-containing nitroimidazole complex for imaging hypoxia: synthesis, characterization, and xanthine oxidase-catalyzed reduction. *J Med Chem.* 1994;37:9-17.
9. Linder K, Cyr J, Chan Y, et al. Effect of substituents on physicochemical and biological behavior of Tc-PnAO nitroimidazoles [abstract]. *J Nucl Med.* 1994;35(suppl):18P.
10. Albert JS. The potential for myocardial imaging with hypoxia markers. *Semin Nucl Med.* 1999;29:330-338.
11. Brown JM, Yu NY, Brown DM, Lee WW. SR-2508: a 2-nitroimidazole amide which should be superior to misonidazole as a radiosensitizer for clinical use. *Int J Radiat Oncol Biol Phys.* 1981;7:695-703.
12. Coleman CN, Wasserman TH, Urtasun RC, et al. Final report of the phase I trial of the hypoxic cell radiosensitizer SR2508 (etanidazole) Radiation Therapy Oncology Group 83-03. *Int J Radiat Oncol Biol Phys.* 1990;18:389-393.
13. Shibamoto Y, Nishimoto S, Shimokawa K, et al. Characteristics of fluorinated nitroazoles as hypoxic cell radiosensitizers. *Int J Radiat Oncol Biol Phys.* 1989;16:1045-1048.
14. Rasey JS, Hofstrand PD, Chin LK, Tewson TJ. Characterization of [^{18}F]fluoroetanidazole, a new radiopharmaceutical for detecting tumor hypoxia. *J Nucl Med.* 1999;40:1072-1079.
15. Melo T, Duncan J, Ballinger JR, Rauth AM. BRU59-21, a second-generation $^{99\text{m}}\text{Tc}$ -labeled 2-nitroimidazole for imaging hypoxia in tumors. *J Nucl Med.* 2000;41:169-176.
16. Sasai K, Shibamoto Y, Takahashi M, et al. A new, potent 2-nitroimidazole nucleoside hypoxic cell radiosensitizer, RP170. *Jpn J Cancer Res.* 1989;80:1113-1118.
17. Wada H, Iwata R, Ido T, Takai Y. Synthesis of 1-[2- ^{18}F]fluoro-1-(hydroxymeth-

- yl)-ethoxy)methyl-2-nitroimidazole (^{18}F)]FENI), a potential agent for imaging hypoxic tissues by PET. *J Label Compd Radiopharm.* 2000;43:785–793.
18. Yamane Y, Ishide N, Kagaya Y, et al. Quantitative double-tracer autoradiography with tritium and carbon-14 using imaging plates: application to myocardial metabolic studies in rats. *J Nucl Med.* 1995;36:518–524.
 19. Fukuchi K, Kusuoka H, Watanabe Y, Fujiwara T, Nishimura T. Ischemic and reperfused myocardium detected with technetium-99m-nitroimidazole. *J Nucl Med.* 1996;37:761–766.
 20. Chida M, Kagaya Y, Imahori Y, et al. Visualization of myocardial phosphoinositide turnover with 1-[^{14}C]-butyryl-2-palmitoyl-rac-glycerol in rats with myocardial infarction. *J Nucl Med.* 2000;41:2063–2068.
 21. Yamane Y, Ishide N, Kagaya Y, et al. Stimulated glucose uptake in the ischemic border zone: its dependence on glucose uptake in the normally perfused area. *J Nucl Med.* 1997;38:1515–1521.
 22. Vivaldi MT, Kloner RA, Schoen FJ. Triphenyltetrazolium staining of irreversible ischemic injury following coronary artery occlusion in rats. *Am J Pathol.* 1985;121:522–530.
 23. Johnson LL, Schofield L, Donahay T, Mastrofrancesco P. Myocardial uptake of a $^{99\text{m}}\text{Tc}$ -nitroheterocycle in a swine model of occlusion and reperfusion. *J Nucl Med.* 2000;41:1237–1243.
 24. Lehninger A, Nelson D, Cox M. *Principles of Biochemistry.* 2nd ed. New York, NY: Worth Publishers; 1993.
 25. Liedtke AJ. Alterations of carbohydrate and lipid metabolism in the acutely ischemic heart. *Prog Cardiovasc Dis.* 1981;23:321–336.
 26. Camici P, Ferrannini E, Opie LH. Myocardial metabolism in ischemic heart disease: basic principles and application to imaging by positron emission tomography. *Prog Cardiovasc Dis.* 1989;32:217–238.
 27. Schwaiger M, Schelbert HR, Ellison D, et al. Sustained regional abnormalities in cardiac metabolism after transient ischemia in the chronic dog model. *J Am Coll Cardiol.* 1985;6:336–347.
 28. Rosamond TL, Abendschein DR, Sobel B, et al. Metabolic fate of radiolabeled palmitate in ischemic canine myocardium: implications for positron emission tomography. *J Nucl Med.* 1987;28:1322–1329.
 29. Sun D, Nguyen N, DeGrado TR, Schwaiger M, Brosius FC III. Ischemia induces translocation of the insulin-responsive glucose transporter GLUT4 to the plasma membrane of cardiac myocytes. *Circulation.* 1994;89:793–798.
 30. Slot JW, Geuze HJ, Gigengack S, James DE, Lienhard GE. Translocation of the glucose transporter GLUT4 in cardiac myocytes of the rat. *Proc Natl Acad Sci USA.* 1991;88:7815–7819.
 31. Zaninetti D, Greco-Perotto R, Assimacopoulos-Jeannet F, Jeanrenaud B. Effects of insulin on glucose transporters in rat heart. *Biochem J.* 1988;250:277–283.
 32. Watanabe T, Smith MM, Robinson FW, Kono T. Insulin action on glucose transport in cardiac muscle. *J Biol Chem.* 1984;259:13117–13122.
 33. Wheeler TJ. Translocation of glucose transporters in response to anoxia in heart. *J Biol Chem.* 1988;263:19447–19454.
 34. Rattigan S, Appleby GJ, Clark MG. Insulin-like action of catecholamines and Ca^{2+} to stimulate glucose transport and GLUT4 translocation in perfused rat heart. *Biochim Biophys Acta.* 1988;1094:217–223.
 35. Zaninetti D, Greco-Perotto R, Jeanrenaud B. Heart glucose transport and transporters in rat heart: regulation by insulin, workload and glucose. *Diabetologia.* 1988;31:108–113.
 36. Camps M, Castello A, Munoz P, et al. Effect of diabetes and fasting on GLUT-4 (muscle/fat) glucose-transporter expression in insulin-sensitive tissues. *Biochem J.* 1992;282:765–772.
 37. Morgan HE, Cadenas E, Regan DM, et al. Regulation of glucose uptake in muscle. II. Rate-limiting steps and effects of insulin and anoxia in heart muscle from diabetic rats. *J Biol Chem.* 1961;236:262–268.

